PROCEEDINGS, Seventeenth Workshop on Geothermal Reservoir Engineering
Stanford University, Stanford, California, January 29-31, 1992
SGP-TR-141

PRELIMINARY RESERVOIR ENGINEERING STUDIES OF THE MIRAVALLES GEOTHERMAL FIELD, COSTA RICA

C. Haukwa,[1] G. S. Bodvarsson,[1] M. J. Lippmann[1] and A. Mainieri[2]

[1]Earth Sciences Division
Lawrence Berkeley Laboratory
Berkeley, CA 94720

[2]Instituto Costarricense de Electricidad
San Jose, Costa Rica

ABSTRACT

The Earth Sciences Division of Lawrence Berkeley Laboratory in cooperation with the Instituto Costarricense de Electricidad is conducting a reservoir engineering study of the Miravalles geothermal field, Costa Rica. Using data from eight exploration wells, a two-dimensional areal, natural-state model of Miravalles has been developed. The model was calibrated by fitting the observed temperature and pressure distributions and requires a geothermal upflow zone in the northern part of the field, associated with the Miravalles volcano and an outflow towards the south. The total hot (about 260°C) water recharge is 130 kg/s, corresponding to a thermal input of about 150 MWt.

On the basis of the natural-state model a two-dimensional exploitation model was developed. The field has a production area of about 10 km^2, with temperatures exceeding 220°C. The model indicated that power generation of 55 MWe can be maintained for 30 years, with or without injection of the separated geothermal brine. Generation of 110 MWe could be problematic. Until more information becomes available on the areal extent of the field and the properties of the reservoir rocks, especially their relative permeability characteristics, it is difficult to ascertain if 110 MWe can be sustained during a 30-year period.

INTRODUCTION

Eight deep wells, with depths varying between 1162 and 2270 m, have been drilled at the Miravalles geothermal field (Figures 1 and 2) and the construction of a 55 MWe power plant is underway (Alvarado, 1987; Mainieri and Vaca, 1990). The field is located within a Pleistocene volcanic caldera. The Miravalles volcano itself, northeast of the wellfield, is a post-caldera feature that developed on the caldera rim.

The successful wells have been completed at the intersection of west-east and north-south trending faults (Mainieri et al., 1985). The lithology of the area consists of a series of volcanic flows and pyroclastic units. Geothermal fluids are produced from fractures, mainly in the so-called "basement" which is comprised of crystal-lithic tuffs, andesitic lavas and welded tuffs (Mainieri et al., 1985). Details on the geologic characterists of the area can be found in ICE-ELC (1988) and Mora (1988, 1989).

Analysis of the available well log and well test data was carried out in order to characterize the physical and thermodynamic properties of the reservoir, as well as to develop a conceptual model of the field. Then, following a general approach to evaluate such systems (Bodvarsson and Witherspoon, 1989), natural state and exploitation models of the Miravalles system were developed and used to study the power generation potential of the field.

RESERVOIR ENGINEERING STUDIES

Initial Temperature Distribution

Figure 3 (ICE-ELC, 1988) presents E-W and NNE/SSW geologic sections, as well as the temperature

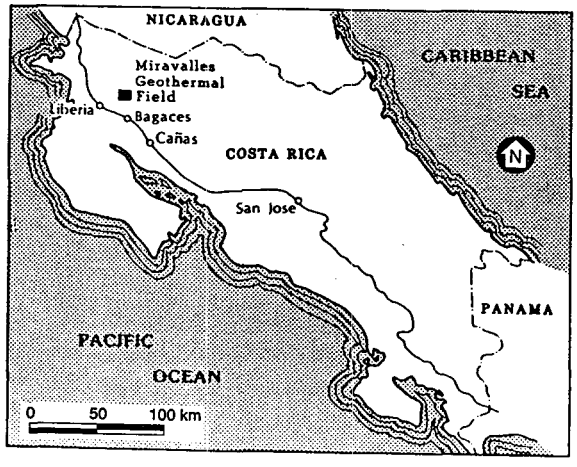

Figure 1. Location of the Miravalles geothermal field.

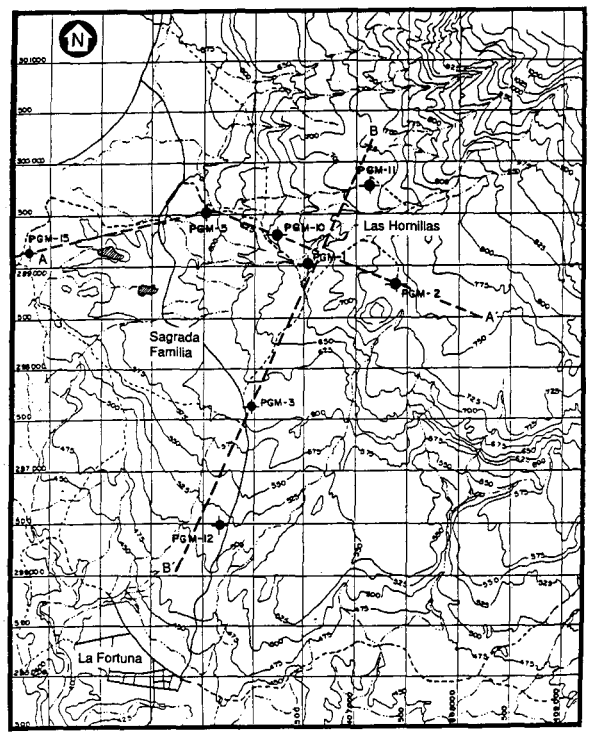

XBL 9112-6887

Figure 2. Location of Miravalles wells and cross-sections shown in Figure 3.

distribution in Miravalles; the location of the sections is given in Figure 2. On the basis of the isotherms shown in the E-W section (Figure 3a), the center of the convective plume is considered to be around wells PGM-1 and 10, with temperatures decreasing towards the west, and then falling steeply about 1 km west of PGM-5. The eastern limit of the field is indicated by the strong thermal inversion observed in PGM-2.

The NNE-SSW section (Figure 3b) shows higher temperatures to the north with the highest (exceeding 255°C) near PGM-11 at approximately −250 to −450 masl. Below that elevation downhole logs in PGM-11 indicate a reversal with temperature decreasing to 245°C at −550 masl. The inferred sharp temperature drop west of PGM-3 is likely distorted by the strong internal wellbore flow that masks the true temperatures. Therefore, the actual 235 and 245°C isotherms are probably more gradual than depicted in Figure 3b.

Fluid-inclusion studies suggest that temperatures in parts of the field were significantly warmer in the past. Homogenization temperatures for liquid-rich fluid inclusions were up to about 70°C hotter than those measured at some sampled depths (Bargar and Fournier, 1988).

Temperature logs for Miravalles wells PGM-1, 2, 3, 5, 10, 11, 12 and 15 were analyzed to obtain the initial (pre-exploitation) state temperature distribution at the reference elevation of −200 masl. The logs show a nearly uniform reservoir top at an elevation of 200-250 masl over the central part of the field, but dropping steeply to the west (towards PGM-15) and gradually to the south. The measurements show that at an elevation of −200 masl the temperature is highest around well PGM-11 (above 240°C), with isotherms elongated in a SSW direction (Figure 4). This temperature distribution corresponds approximately with the heat flow maps developed by Koenig (1980) and indicates an upflow region in the area of PGM-11, 10 and 1, and outflow south of PGM-12; this agrees with the model of Grigsby et al. (1989). The sharp drop of temperature towards PGM-15 suggests a hydrological barrier or cold water encroachment from the west.

Initial Pressure Distribution

Downhole pressure logs data obtained in the Miravalles wells were analyzed to obtain pressures at −200 masl, an elevation where all the wells except PGM-15 show permeability. The pressure logs taken in 1988-1989 following long periods of recovery, are believed to best represent the undisturbed reservoir pressure. However, many of the wells have internal flow which masks true reservoir pressures.

The measured pressure distribution at −200 masl (Table 1, Figure 5) shows the highest pressure in PGM-11 (51 bar), fairly uniform pressure around PGM-1, 2 and 10, and a general gradient toward the SSW over the wellfield. To the west, beyond PGM-5, the pressure distribution is not well defined due to lack of subsurface data. Southward the pressure drops gradually at about 1 bar/km. This pressure distribution combined with the corresponding temperature distribution indicates that the outflow zone for the geothermal system is towards the south, perhaps associated with the Bagaces hot springs (see Figure 6) and other surface manifestations to the south.

Well Tests

A number of injection and production tests were performed to obtain the hydraulic and production characteristics of the wells and reservoir. Transient injection and fall-off tests were carried out in wells PGM-2, 10, 11, 12 and 15. The results are summarized in Table 1. All were short-duration tests (typically less than 1-1/2 hour) and pressures did not stabilize. In PGM-15, even long injection steps of up to 6 hours did not result in stable pressure due to low formation permeabilities.

Pressure profiles measured in PGM-1, 2, 3, 5, 10 and 12 during flow were used to obtain well productivity indices (Table 1). No measurable drawdown was observed in PGM-1 and 3, indicating very high reservoir permeability.

Variable flow discharge tests were performed in PGM-1, 3, 5, 10 and 11. These tests referred to as Reservoir Characterization Curves (RCC), were used to obtain

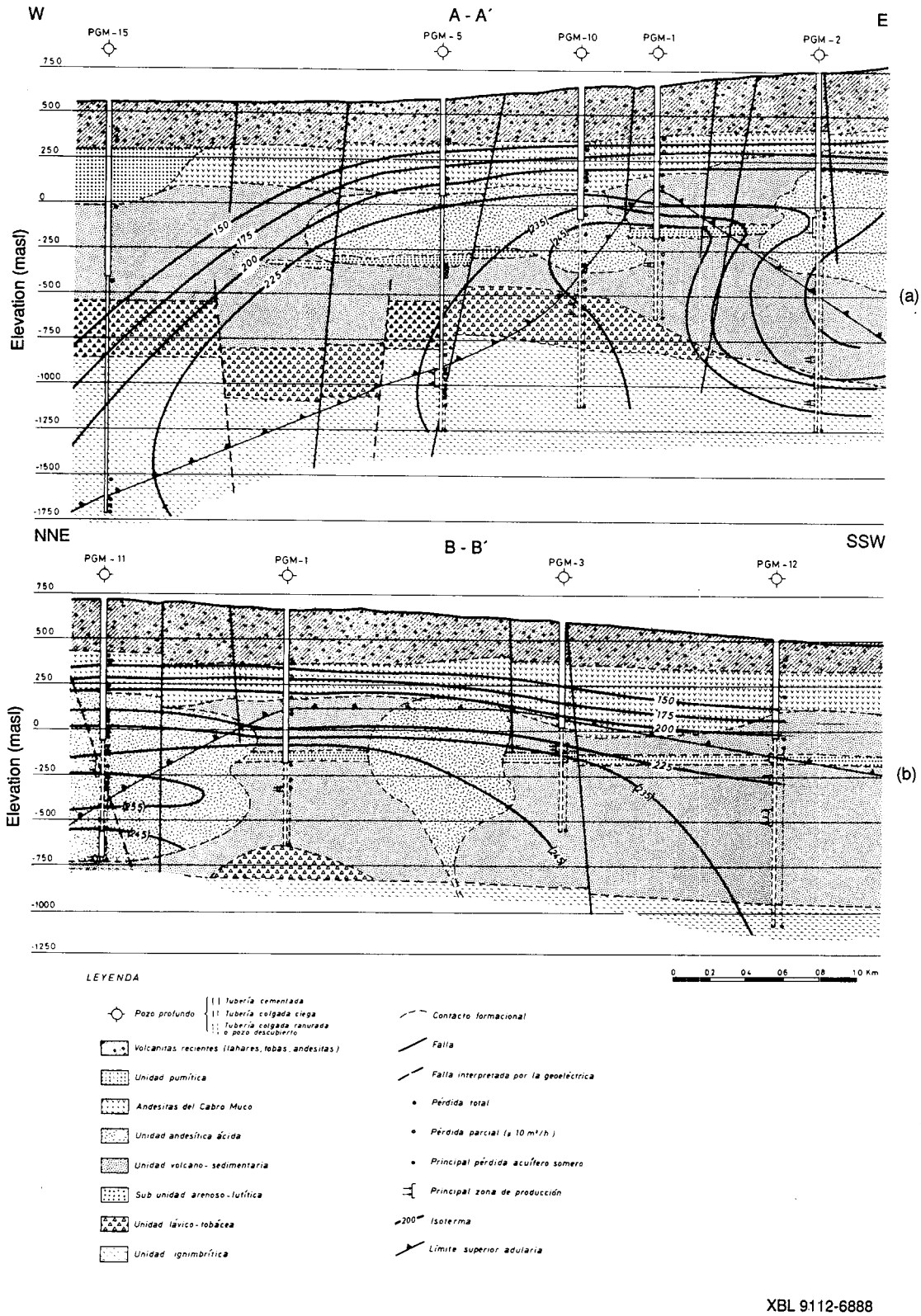

Figure 3. Geologic sections and temperature distribution in the Miravalles field (from ICE-ELC, 1988).

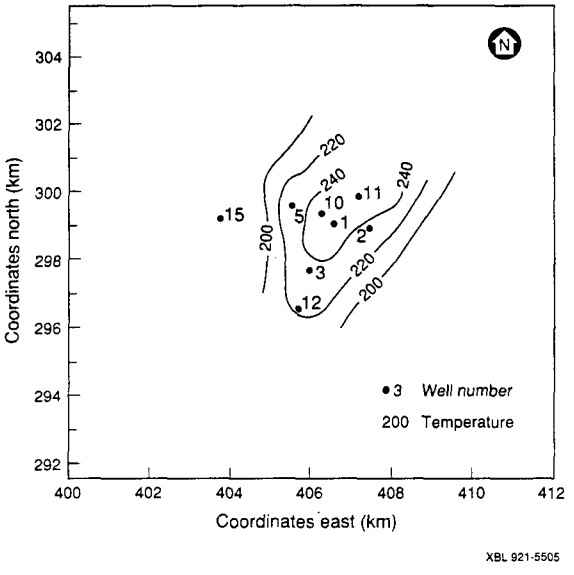

Figure 4. Measured temperature distribution at −200 masl (in °C)

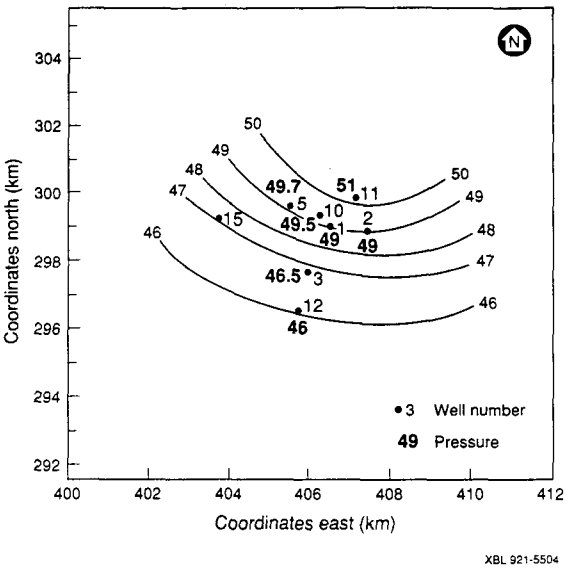

Figure. 5. Measured pressure distribution at −200 masl (in bar)

Table 1. Characteristics of Miravalles Wells

Well No.	Injectivity Index (kg/s/bar)	Productivity Index (kg/s/bar)	Flow Rate[a] (kg/s)	Enthalpy[a] (kJ/kg)	Power[a] (MWe)	Temperature at -200 masl (°C)	Pressure at -200 masl (bar)
1.	-	-	70.0	1050	5.5	250	49.0
2.[b]	2.4	0.3(10.0[c])	60.8	1040	4.6	235	49.0
3.	-	-	90.0	1040	6.9	240	46.5
5.	-	6.0(3.0[d])	65.0	1030	4.8	230	49.7
5.	-	0.7–3.5[e]					
10.[f]	1.0	1.5(0.6)	28.0	1030	2.1	250	49.5
11.	3.3-4.2	-	65.0	1100	5.7	255	51.0
12.	10.0	11.2	135.0	1030	10.0	235	46.0
15.	0.6	-	-	-	-	102	-
		TOTAL	513.8		39.6		

Notes
a. Flow rate, enthalpy and power correspond to 10 bar WHP.
b. After deepening, it produced acid fluid (pH 2.2).
c. After the well was deepened.
d. Repeat test after 50 days of production tests, from flowing pressure profiles. Reduced permeability possibly due to scaling.
e. Increase of productivity index with flow rate, from variable flow test.
f. Transient pressure tests indicate skin damage.

well production characteristics as well as the productivity indices, by monitoring pressure at a single downhole location while the flow rate was changed. No reliable results were obtained for PGM-1, 3, and 11 because the tools were not placed at depths near productive zones. PGM-5 showed an increase in the productivity index with flow rate, from 0.7 to 3.5 kg/s/bar. The well also showed a 50% drop in productivity index following 50 days of discharge. This drop is probably attributable to calcite scaling. PGM-10 indicated skin damage from the pressure recovery following discharge, suggesting the low measured productivity index does not represent the average productivity of the reservoir tapped by this well (Table 1).

The results of the transient and production tests therefore suggest very high permeabilities for wells PGM-1, 2, 3 and 12, and moderate ones for wells PGM-5 and 10. However, due to a high potential for calcite scaling (Granados and Gudmundsson, 1985; Vaca et al., 1989), results of transient pressure tests conducted after prolonged periods of production may not give good indication of undisturbed reservoir permeabilities.

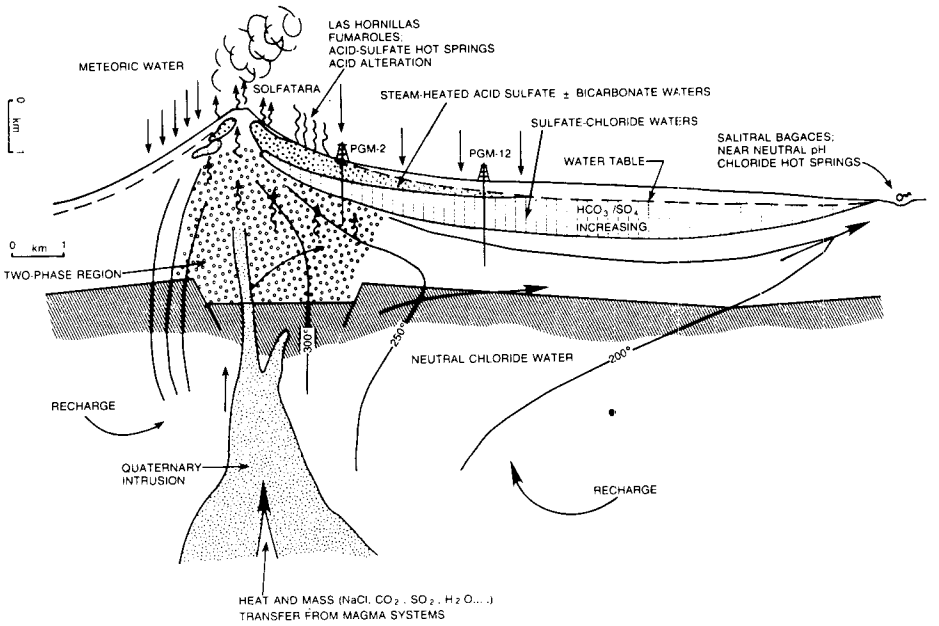

Figure 6. Conceptual model of Miravalles geothermal field (from Grigsby et al., 1989; adapted from Henley and Ellis, 1983).

The production tests show that the wells produce single phase liquid with an average enthalpy of 1045 kJ/kg and that they have capacities that range from 2.1 to 10.0 MWe, at 10 bar wellhead pressure (WHP; Table 1). In PGM-2, when deepened from 1210 to 2000 m, the tests indicated acid fluid production (pH 2.2; Truesdell, 1991). This fluid is produced from feed zones below 1500 m depth (below −760 masl), making the deep zones near PGM-2 unsuitable for production.

In June 1990 began a 92-day interference and tracer test. Well PGM-11 was produced at 36 kg/s, and 32 kg/s of 845 kJ/kg separated brine was injected into well PGM-2. The pressure drawdown was measured in wells PGM-1 and 5. During this test 63 kg of Iodine-131 tracer was injected into PGM-2 and tracer returns sampled in PGM-3, 10, 11 and 12. From the tests the maximum pressure drawdown in PGM-1 and 5 was only 0.2 bar and the pressure showed large fluctuations attributable to instrument errors or unstable reservoir pressures. The measured tracer velocities were 350 m/day at PGM-3, 150 m/day at PGM-12 and 100 m/day at PGM-10. No tracer return was measured at PGM-11, indicating either a hydraulic barrier between PGM-11 and 2 or a level of production/injection insufficient to reverse the general north-south pressure gradient.

Conceptual Model

The observed temperature and pressure distributions (Figures 3-5) suggest that the heat source for the geothermal system is related to the Miravalles volcano, which is centered about 4.5 km northeast of PGM-11. As deep circulating meteoric waters are heated and rise, they form a two-phase boiling zone (≥ 250 °C) centered in the reservoir in the area of wells PGM-1, 2, 10 and 11. Some geothermal fluid is discharged at the surface through fumaroles and acid sulfate hot springs located in the northern part of the field. The majority of the fluid however, flows to the south and manifests itself as near neutral-pH chloride hot springs. A schematic representation of this hydrogeological model is shown in Figure 6 (from Grigsby et al., 1989).

Natural-State Model

As a first step in constructing a detailed three-dimensional exploitation model for Miravalles, a two-dimensional areal, natural-state model was developed. A natural-state model of a geothermal area, gives quantitative estimates of the heat and mass throughput in the system. It should ideally reproduce the observed temperature and pressure distributions and give global estimate of reservoir permeability. Most geothermal reservoirs exhibit a high degree of fracture control of permeability in which thin, highly conductive channels (i.e faults and fractures) transmit most of the fluid.

Based on the observed temperature and pressure distributions the two-dimensional horizontal natural state model was centered at an elevation of −200 masl, with a uniform thickness of 1000 m (i.e., top of the model at 300 masl; bottom at −700 masl). The model is about 96 km wide in the E-W direction and about 112 km long in the N-S direction. This large areal extent was used so that no boundary effects would be felt when simulating the exploitation of the field. For the 12 km × 14 km central part of the field (Figure 7), conductive heat loss

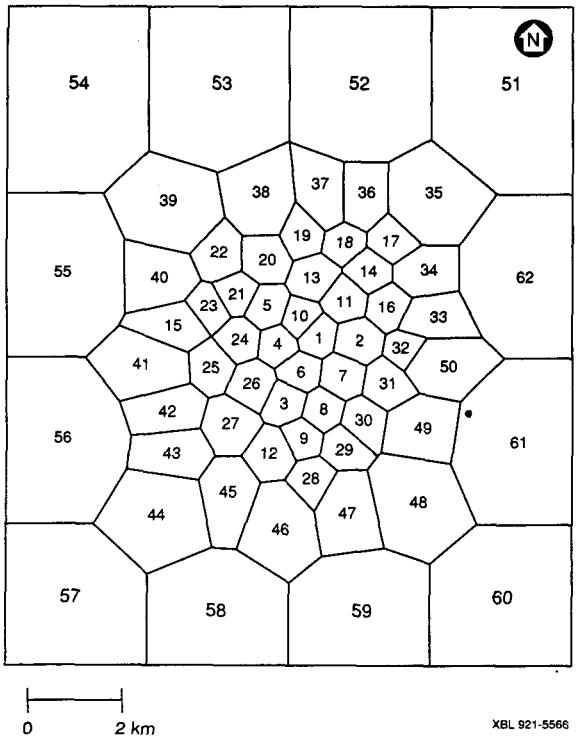

Figure 7. Two-dimensional mesh used for the natural and exploitation state models. (mesh elements 1, 2, 3, 5, 10, 11, 12 and 15 are centered on the deep exploration wells)

to a constant 20°C surface was allowed in the model. The vertical distances between the model nodes and the surface were based on the estimated depth to the reservoir top.

The formation properties used were: density 2600 kg/m^3, porosity 6%, thermal conductivity 3 W/m/°C and specific heat capacity 1000 J/kg/°C. The permeability was initially selected based on the values used in the modeling studies by ICE-ELC (1988). These permeabilities were then adjusted in order to match the natural state temperature and pressure distributions. An anisotropic porous medium was assumed. Permeability increases of up to two orders of magnitude were required in the direction of the high-permeability faults, to match the observed natural-state temperature distribution. The boundary blocks were modeled simply as low permeability areas. Hot fluid at variable temperatures and rates was injected into elements 11, 13, 14, 16, 17, 18, 34 and 35 (Figure 7). Fluid losses of 0.5 kg/s were allowed through elements 2, 5 and 45 to represent surface manifestation discharge. Element 58 to the south was selected as the natural fluid sink, with fluid extracted at a rate q proportional to a specified productivity index PI and against a specified downhole pressure P_{wb} according to the following formula,

$$q_\beta = \frac{k_{r\beta}}{\mu_\beta} \rho_\beta \, PI \, (P_\beta - P_{wb})$$

Where $k_{r\beta}$ is the relative permeability, μ_β is the viscosity and ρ_β is the density of each phase β. Linear relative permeability curves were used with residual liquid and vapor saturations of 25% and 1%, respectively.

The numerical simulation was carried out using the multiphase, multidimensional code TOUGH2 (Pruess, 1990), and run through a simulation time of about 2 million years. The calculated steady-state temperature and pressure distributions were compared to measured values (Figures 4 and 5, respectively). The permeabilities and the flow rates were then adjusted until a reasonable match was obtained with the observed natural-state pressure and temperature distributions. The permeabilities needed to match these distributions are shown in Figure 8. The highest permeability are in the element corresponding to PGM-12 and a general N-S high-permeability zone exists across the field indicating that the north-south fault system controls the fluid flow in the system.

Using the 200 and 240°C isotherms as references, the best match to the measured temperature distribution (Figure 9) is obtained using a total recharge of 130 kg/s of 1140 kJ/kg fluid (at about 260°C), representing a thermal through-flow of about 150 MWt. Figure 10 shows the computed natural-state pressure distribution for this model. The calculated N-S pressure gradient matches well the measured pressures in the northern part of the field. The match in the south and on the east-west section is rather poor. However, considering the uncertainties in the measured pressure caused by internal borehole flow, this match was considered to be adequate.

Exploitation model

In order to estimate the generating capacity of the Miravalles field and evaluate its response to different production-injection scenarios, a lumped-wellfield exploitation model (Bodvarsson and Witherspoon,

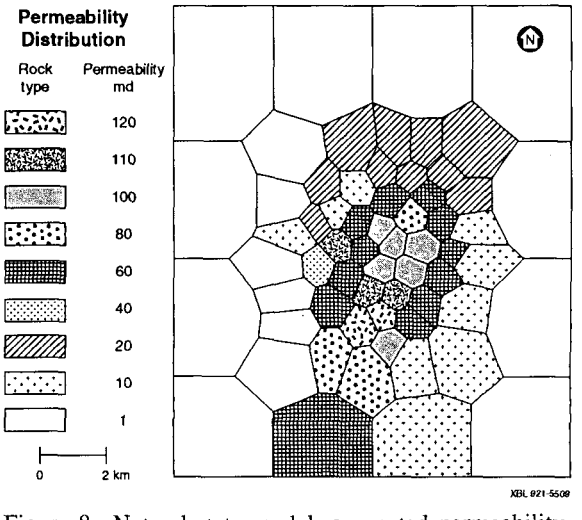

Figure 8. Natural-state model, computed permeability distribution.

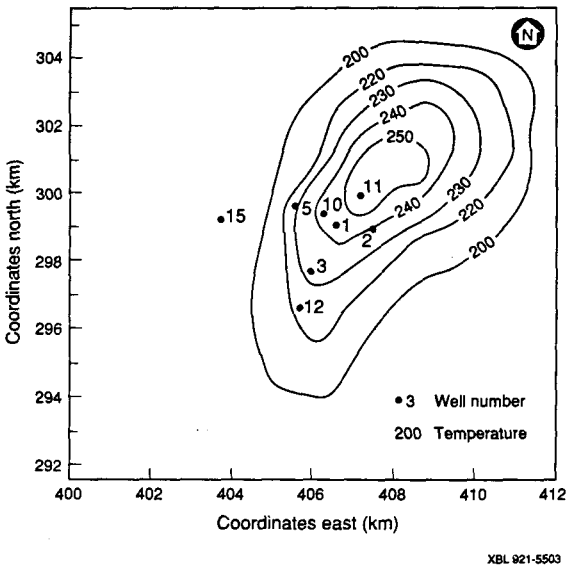

Figure 9. Best model. Computed natural-state temperature distribution at –200 masl (in °C).

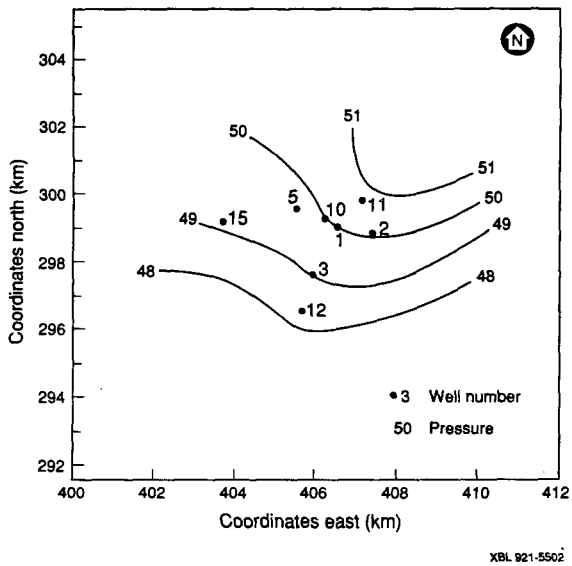

Figure 10. Best model. Computed natural-state pressure distribution at –200 masl (in bar).

1989) was developed. The computational mesh, formation properties, boundary and initial conditions used in the exploitation model were based on those of the natural-state model. The production area was assumed to be within the region enclosed by the 220°C isotherm (Figures 4 and 9). This 10 km^2 area includes seven of the deep exploration wells drilled in the field (not PGM-15) and is represented roughly in the model by elements 1 to 14 and 16 (Figure 11). In PGM-2 only the shallow (normal) production zone was included in the simulation since the bottom of the mesh is at –700 masl.

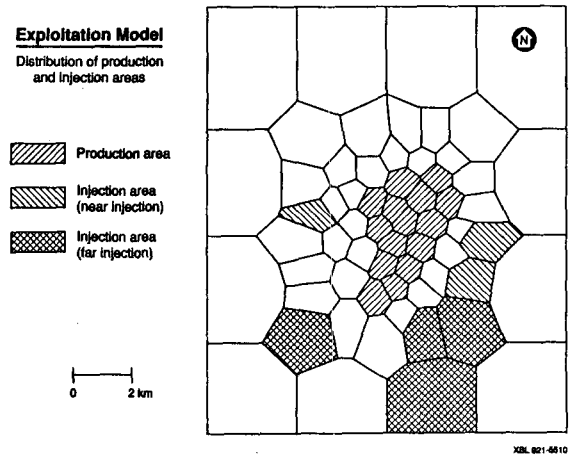

Figure 11. Distribution of production and injection areas in the model (element numbers are given in Figure 7).

As an initial calibration of the exploitation model, the drawdown observed during the June 1990 interference test was matched. The test was modeled by extracting 36 kg/s from element 11 and injecting 32 kg/s into element 2 and computing the pressure changes in elements 1 and 5. To match both the natural-state temperature and pressure distributions and the pressure drop observed in PGM-1 and 5 during the test, required to center of the upflow in element 17, (1.5 km north-east of element 11; Figure 7).

PRELIMINARY RESERVOIR PERFORMANCE STUDIES

Based on projected power development options for Miravalles, the model was used to simulate power production of 55 MWe and 110 MWe for 30 years, with and without injection (a power plant conversion of 2.5 kg/s of steam per MWe was assumed in the calculations). To achieve these levels of electricity generation over that period of time, up to a total of 75 production and make-up wells were placed in elements 1 to 16 (excluding element 15; Figure 7). At the end of the 30 years, most of these elements had an average well density of 8 wells/km^2.

Because at Miravalles the separated fluid must be injected, we examined two injection options: near injection for pressure support and far injection for fluid disposal. Based on the natural-state pressure gradients, injection in the northern part of the field was not considered because of the potential for rapid return of the injected fluid into the production wellfield. Therefore, a main injection area to the east and southeast of PGM-2 was selected (Figure 11). In the model, this area corresponds to elements 47, 48, 49, 50 and 59. Elements 28 to 33 separate the production field from the main injection area. In addition, because of the low permeability in PGM-15 above –700 masl, only small

injection rates were allocated to elements 15 and 44 to the west and south-west of the production field.

The effect of injection for pressure support was investigated by assuming high injection rates into elements 47, 48, 49 and 50; for fluid disposal the high-rate injection was into elements 44, 47, 48 and 59, which are closer to the natural outflow area in the system. In all cases the total injection rate was calculated as a percentage of the total mass produced. The percentages used were 90%, 80%, 50% and 0%. A constant injection enthalpy of 676 kJ/kg, corresponding to hot separated water at about 160°C was assumed.

Production/Injection Simulation

A slightly modified version of TOUGH2 (Pruess, 1990) was used in the study of different production and injection scenarios. For production, a constant productivity index was assigned to each well. The indices used were derived based on data from flowing pressure profiles and calculated or assigned permeability in the elements. The productivity indices ranged between 4.5×10^{-12} and 9.0×10^{-12} m^3, and were conservatively assigned based on the low measured values and on observed well production data.

The computed production rates under the above conditions will depend on the specified flowing bottomhole pressure (PWB) in the well. This pressure as observed from flowing pressure profiles, depends on the flow rate, well geometry and the produced fluid density (which is a function of enthalpy). When production causes pressure drawdown and boiling, it results in decreased flow and increased enthalpy. Therefore, keeping a high fixed PWB will unnecessarily throttle well flow. On the other hand, assuming a low fixed PWB and thus underestimating the hydrostatic component, results in excessively high early-time production rates.

To account for wellbore pressure variations, a wellbore simulator (Aunzo et al., 1991), was used to obtain curves for flowing bottom hole pressure as a function of enthalpy and flow rate, assuming a fixed well geometry. In this model the Armand (1945) correlations were used for prediction of the two-phase pressure drop, because it gives monotonically varying pressures at all flows and enthalpies in contrast to the Orkiszewski (1967) correlations. To correct for PWB variations, the flow rate and enthalpy at a given time step was used to calculate PWB, which was then used to compute the flow rate at the next time step.

In all cases the reservoir performance calculations assumed constant (20 or 30 bar) or variable PWB and examined injection near or far away from the production area. In the former case, because of thermal breakthrough (i.e., lower average enthalpies and steam rates per well) a large number of producers are needed to supply the total required steam rate. The variable PWB cases were found to give more realistic wellbore flow conditions over the 30-year period and are presented below. The effects the relative permeability functions on the results were also examined.

RESULTS OF PERFORMANCE PREDICTION STUDIES

55 MWe Generation

With near injection. The results for this case are shown in Figures 12 and 13. Sufficient steam for 55 MWe is available for 30 years with and without injection. For the 0% injection case the initial average enthalpy of 1100 kJ/kg increases to 1600 kJ/kg after 30 years (Figure 12). For 80% and 90% near injection, the production enthalpy initially rises to 1250 kJ/kg and then declines to 1150-1200 kJ/kg between 10 and 30 years Figure 12). The total number of production wells required over the 30-year period varies from 24 for no injection to 27 for 90% injection (Figure 13).

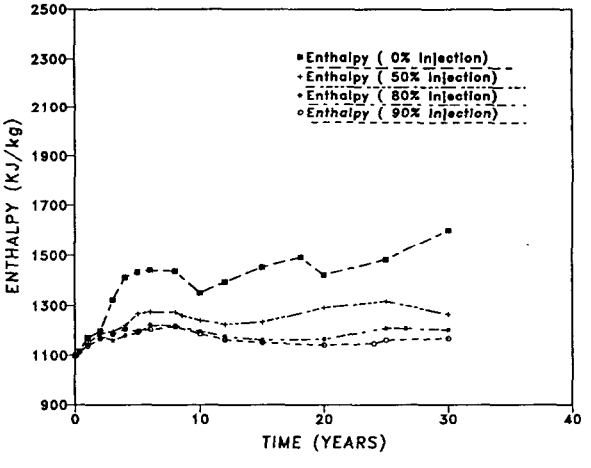

Figure 12. 55 MWe, near injection case. Enthalpy history.

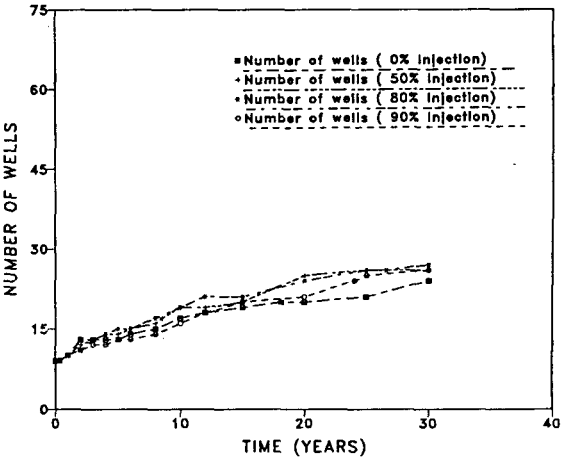

Figure 13. 55 MWe, near injection. Number of required production wells.

With far injection. Figures 14 and 15 show the results for this case. As in the previous case of 55 MWe with near injection, sufficient steam is produced to generate 55 MWe for 30 years with or without injection. However, because there is only a limited thermal impact on the production area, the 80% and 90% injection cases give nearly identical results, with an average produced fluid enthalpy of 1160-1250 kJ/kg, compared to about 1450-1600 kJ/kg for the case of no injection (Figure 14). The number of production wells required over the 30-year period is 27 for both 80% and 90% injection (Figure 15), similar to the near injection case, indicating limited sensitivity to the location of injection wells within the selected injection area.

110 MWe Generation

With near injection. In all cases sufficient steam can be produced to generate 110 MWe during the 30-year period. With 50% injection, the maximum average enthalpy drops to about 1400 kJ/kg (Figure 16) and the total number of production wells reaches 66 at the end of the 30-year period (Figure 17). For the cases of 80% and 90% injection the number production wells rises to 69 and the maximum average enthalpy declines to 1250 kJ/kg for 80% injection and 1200 kJ/kg for 90% injection due to increased return of injected fluid and earlier thermal breakthrough. For the case without injection, rapid pressure drawdown is experienced and production enthalpy rises to 2380 kJ/kg due to boiling within the reservoir (Figure 16). This case requires a total of 53 production wells during the 30-year period (Figure 17).

Therefore, although 110 MWe can be supported over the entire period, a high percentage of injection can be detrimental due to reservoir temperature decline, especially in the areas nearest to the injectors.

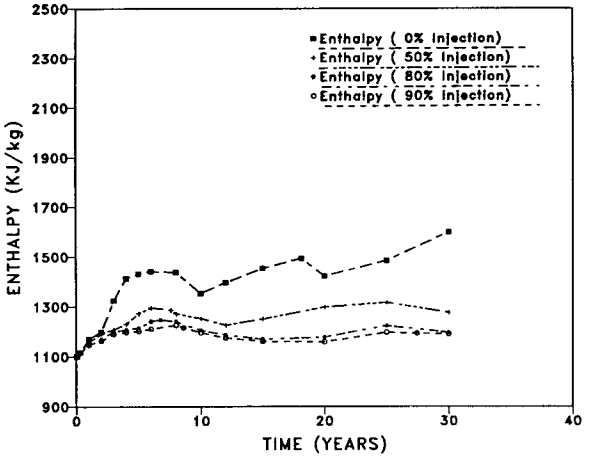

Figure 14. 55 MWe, far injection. Enthalpy history.

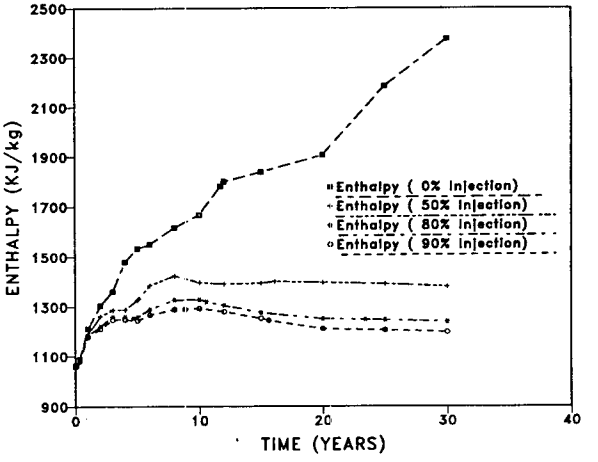

Figure 16. 110 MWe, near injection. Enthalpy history.

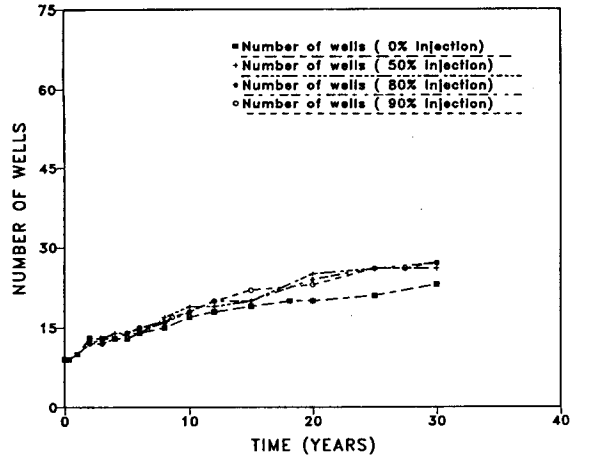

Figure 15. 55 MWe, far injection. Number of required production wells.

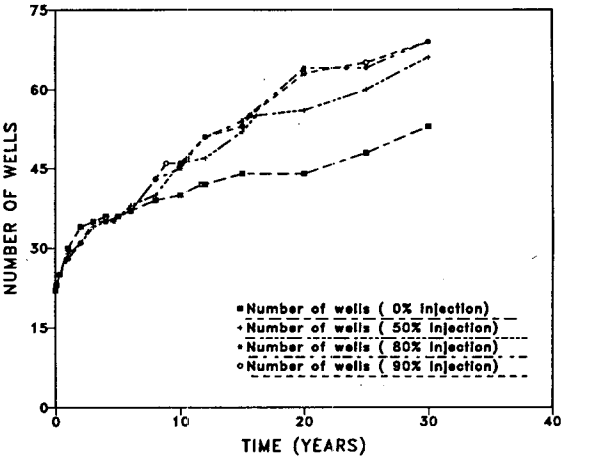

Figure 17. 110 MWe, near injection. Number of required production wells.

With far injection. In all cases with and without injection sufficient steam is produced to generate 110 MWe for 30 years. Injection rates of 80% and 90% have nearly identical effects. The production enthalpy rises to a maximum of 1350 kJ/kg at 12 years, after which the cooling effect of the injected fluid causes the produced enthalpy to drop to an average of 1255 kJ/kg between 20 and 30 years (Figure 18). The total number of required production wells is 67 for 80% injection and 69 for 90% injection (Figure 19).

Thus, even with far injection mainly in the south, there is sufficient pressure support to prevent large-scale reservoir boiling, although individual wells in the north show localized boiling (e.g., enthalpies of up to 1800 kJ/kg for wells located in mesh element 11). Since large-scale boiling may lead to formation scaling due to calcite precipitation, 110 MWe with far injection does not seem to be a feasible alternative for Miravalles. Thermal breakthrough and reservoir boiling with associated scaling, could reduce the total steam production below the required levels.

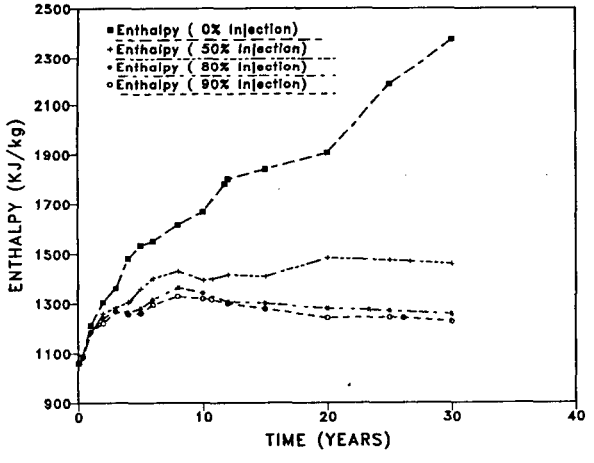

Figure 18. 110 MWe, far injection. Enthalpy history.

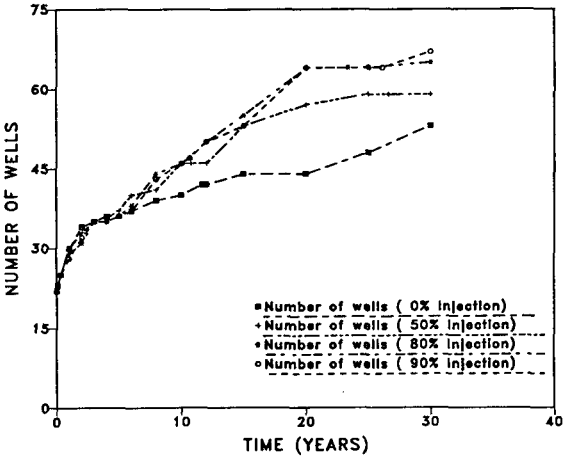

Figure 19. 110 MWe, far injection. Number of required production wells.

Effect of Relative Permeability Functions

In all the cases discussed above linear relative permeability curves were used, with residual saturations of 25% for the liquid and 1% for the vapor. The choice of given relative permeability functions should ideally be based on the observed produced vapor-liquid ratio and the relative saturation of the phases in the reservoir.

Since no such data exist for Miravalles, there is no definite criteria for selecting particular relative permeability curves. Until such data are available it is only possible to perform a sensitivity analysis by evaluating the impact of the relative permeability function on the performance predictions. For example, when Corey relative permeability curves were used with residual saturations of 25% for the liquid and 5% for the vapor, the results showed that generation of 110 MWe could only be supported assuming far injection, with injection rates less than 50%. For the 50% case, a total of 75 wells were required compared to 57 when using the linear relative permeability curves, indicating that the results are very sensitive to the assumed relative permeability functions. It should also be pointed out here that the effects of production/injection cannot be fully analyzed using a two-dimensional areal model. Development of a 3-D model that will take into account the effects of vertical permeability, gravity and depth of injection/production, will give a more realistic prediction of the evolution of the reservoir during exploitation.

CONCLUSIONS AND RECOMMENDATIONS

Eight deep exploration wells at Miravalles have confirmed the presence of a 10 km^2 liquid-dominated geothermal reservoir with temperatures between 220 and 260 °C; the highest temperatures and pressures found in the northern part of the field.

The upflow zone for this system, with a recharge estimated at 150 MWt, is north of PGM-11 and is related to the Miravalles volcano. The main outflow is found to the south, perhaps associated with the Bagaces hot springs (Figure 6). Permeability within the field is controlled by the north-south and the east-west fault systems, with the former dominating. Individual wells produce enough steam to generate 2.1 to 10 MWe, at 10 bar WHP.

The study indicates that at Miravalles the known system can reliably support a power generation of 55 MWe over a period of 30 years, and that a total of 24 to 28 production wells may be required contingent on the type of injection operation that is implemented.

Generation of 110 MWe for 30 years appears possible; 53 to 70 producers may be needed depending on the location of the injection wells and the rate of injection. However, there might be potential problems related to thermal breakthrough and formation scaling. Since these predictions strongly depend on assumed relative

permeability functions, information on an initial 55 MWe development should be used to re-evaluate the response of the field to 110 MWe production.

A high rate of injection for pressure support is required to prevent boiling and minimize calcite scaling within the formation. Based on our model, injection will have to be sited E and SE of PGM-2. A three-dimensional model will give a better indication of the location of injection wells by studying deep and shallow injection.

To prove the existence of high temperatures and pressures to the north and northeast of PGM-11, further wells should be sited in that area.

Since PGM-2 encountered acid fluids after it was deepened, the extent of the acid reservoir should be ascertained by drilling a deep well at about one km east of PGM-2. This proposed well could also be used for injection during the exploitation of the field. The connection between the acid reservoir and the main, shallow reservoir should be ascertained by planning long-term injection tests or by high-rate injection tests in PGM-2.

ACKNOWLEDGEMENTS

We appreciate the technical review by Emilio Antúnez and Norman Goldstein and the production of the paper by Judith Peterson and Ellen Klahn. This work was sponsored by the Los Alamos National Laboratory through a contract from the United States Agency for International Development and was also supported by the U. S. Department of Energy, under contract No. DE-AC03-76SF00098.

REFERENCES

Alvarado J., J. A. 1987. Perforación y mediciones en el proyecto geotérmico Miravalles. Proceedings International Symposium on Development and Exploitation of Geothermal Resources, October 5-9, Cuernavaca, Morelos, Mexico, 159-165.

Armand, A. A., 1945. Resistance to two-phase flow in horizontal tubes (in Russian). Izv. VTI, 1946, 15(1), 16-23.

Aunzo, Z. P., Bjornsson, G. and Bodvarsson, G. S., 1991. Wellbore models GWELL, GWNACL, and HOLA. Lawrence Berkeley Laboratory report LBL-31428.

Bargar, K. E. and Fournier, R. O., 1988. Fluid-inclusion evidence for previous higher temperatures in the Miravalles geothermal field, Costa Rica, *Geothermics, 17* (5/6), 681-693.

Bodvarsson, G. S. and Witherspoon, P. A., 1989. Geothermal reservoir engineering, Part I. *Geothermal Science and Technology, 2*(1), 1-68.

Granados, E. G. and Gudmundsson, J. S., 1985. Production testing in Miravalles geothermal field, Costa Rica. *Geothermics, 14*(4), 525-538.

Grigsby, C. O., Goff, F., Trujillo Jr., P. E., Counce, D. A., Dennis, B., Kolar, J. and Corrales, R., 1989. Results of investigation at the Miravalles geothermal field, Costa Rica, Part 2: Downhole fluid sampling. Los Alamos National Laboratory report LA-11510-MS, Part 2.

Henley, R. W. and Ellis, A. J., 1983. Geothermal systems ancient and modern: A geochemical review. *Earth-Sci. Rev., 19,* 1-50.

ICE-ELC, 1988. Programa de obras de generación; perïodo 1990-1993. Informe de factibilidad. Planta geotérmica de Miravalles, 2da. Unidad. ICE internal report.

Koenig, J. B., 1980. Exploration and discovery of the Miravalles geothermal field, Costa Rica: A case study. Geothermal Resources Council Special Report 9, 59-70.

Mainieri P., A. and Vaca C., L., 1990. Costa Rica: Country update report, *Geothermal Resources Council Trans., 14*(I), 23-29.

Mainieri, A., Granados, E., Corrales, R. and Vaca, L., 1985. Miravalles geothermal field, Costa Rica. Technical report. *Geothermal Resources Council Trans., 9*(I), 279-283.

Mora P., O., 1988. Geologïa de las piroclastitas en los alrededores de Bagaces, Provincia de Guanacaste, Costa Rica. Tesis de licenciatura, Escuela Centroamericana de Geologïa, Universidad de Costa Rica, San José, Costa Rica.

Mora P., O., 1989. Borehole geology and alteration mineralogy of well PGM-5, Miravalles, Guanacaste, Costa Rica. UNU Geothermal Training Programme, Reykjavik, Iceland, Report 5-1989.

Orkiszewski J., 1967. Predicting two-phase pressure drop in vertical pipe. Journal of Petroleum Technology, June 1967, 829-838.

Pruess K., 1990. TOUGH2- A general purpose numerical simulator for multiphase fluid and heat flow. Lawrence Berkeley Laboratory report LBL-29400.

Truesdell, A. H., 1991. Origin of acid fluids in geothermal reservoirs. *Geothermal Resources Council Trans., 15,* 289-296.

Vaca, L., Alvarado, A. and Corrales, R., 1989. Calcite deposition at Miravalles geothermal field, Costa Rica. *Geothermics, 18*(1/2), 305-312.